

Manuscript Number: VOLGEO4734R1

Title: Carbon dioxide diffuse emission and thermal energy release from hydrothermal systems at Copahue-Caviahue Volcanic Complex (Argentina)

Article Type: Research Paper

Keywords: Caviahue Caldera, Copahue Volcano CO2 diffuse degassing, thermal energy.

Corresponding Author: Mrs. María Clara Isabel Lamberti, M.D.

Corresponding Author's Institution: Indean - Conicet

First Author: Giovanni Chiodini, Dr

Order of Authors: Giovanni Chiodini, Dr; Carlo Cardellini, Dr; María Clara Isabel Lamberti, M.D.; Mariano Augusto, Dr; Alberto Caselli, Dr; Caterina Liccioli, Licenciada; Giancarlo Tamburello, Dr; Franco Tassi, Dr; Orlando Vaselli, Dr; Stefano Caliro, Dr

Abstract: The north-western sector of Caviahue caldera (Argentina), close to the active volcanic system of Copahue, is characterized by the presence of several hydrothermal sites that host numerous fumarolic emissions, anomalous soil diffuse degassing of CO₂ and hot soils. In March 2014, measurements of soil CO₂ fluxes in 5 of these sites (namely, Las Máquinas, Las Maquinitas I, Las Maquinitas II, Anfiteatro, and Termas de Copahue) allowed to estimate that ~165 tons of deeply derived CO₂ are daily released. The gas source is likely related to a relatively shallow geothermal reservoir containing a single vapor phase as also suggested by both the geochemical data from the 3 deep wells drilled in the 1980's and gas geoindicators applied to the fumarolic discharges. Gas equilibria within the H-C-O gas system indicate the presence of a large, probably unique, single phase vapor zone at 200-210 °C feeding the hydrothermal manifestations of Las Máquinas, Las Maquinitas I and II and Termas de Copahue. A natural thermal release of 107 MW was computed by using CO₂ as a tracer of the original vapor phase. The magmatic signature of the incondensable fumarolic gases, the wide expanse of the hydrothermal areas and the remarkable high amount of gas and heat released by fluid expulsion seem to be compatible with an active magmatic intrusion beneath this portion of the Caviahue caldera.



Buenos Aires, 30 April 2015

Dear Editor,

We are pleased to submit to the Journal of Volcanology and Geothermal Research the paper titled “Carbon dioxide diffuse emission and thermal energy release from hydrothermal systems at Copahue volcano (Argentina)” by Giovanni Chiodini, Carlo Cardellini, María Clara Lamberti, Mariano Augusto, Alberto Caselli, Caterina Liccioli, Giancarlo Tamburello, Franco Tassi and Orlando Vaselli. All authors have actively contributed to this original work and have seen the final version of the submitted manuscript.

In the manuscript we present and discuss the results of the investigation of diffuse degassing in the north-western sector of Caviahue caldera (Argentina) close to the active volcanic system of Copahue. The area is characterized by anomalous soil diffuse CO₂ degassing, hot soils and fumarolic discharge. We estimated that ~165 tons of deeply derived CO₂ are daily released by a geothermal reservoir containing a single vapor phase with a temperature of ~200-215 °C, as suggested by the geochemical data of the fumarolic discharges and deep wells.

Using CO₂ as a tracer of the original vapor phase, a natural thermal release of ~110 MW was computed for the area.

The magmatic signature of the incondensable fumarolic gases, the large extension of the hydrothermal areas and the remarkable high amount of gas and heat released by fluid expulsion seem to be compatible with an active magmatic intrusion beneath this portion of the Caviahue caldera.

At our best knowledge, it is the first work on diffuse degassing in the area.

We are looking forward to hearing from you and should you need any further detail, please do not hesitate to contact us at the below reported coordinates.

Best Regards.

On the behalf of all the Authors,

Lic. María Clara Lamberti

E-mail: mclamberti@gl.fcen.uba.ar

Instituto de Estudios Andinos Don Pablo Groeber

Departamento de Geología – Facultad de Ciencias Exactas y Naturales
Universidad de Buenos Aires
Pabellón II – Entrepiso – Oficina 29
Ciudad Universitaria (1428) Buenos Aires
+54 11 4576 3400
idean@gl.fcen.uba.ar
<http://www.idean.gl.fcen.uba.ar>



Dear Editor,

We thank you and both the reviewers for the positive comments to our work. The revised version takes into account all the suggestions of the reviewers.

It follows a point to point reply to the main reviewer comments.

Reviewer#1

The reviewer provided just a general comment and some corrections in the text. There are in our opinion some main points:

1) **Estimation of heat flux from soil temperature measurements** (i.e. the method of Fridriksson et al. 2006, and Dawson 1964). We note that this is an empirical method based on the comparison between soil temperature at 15 cm of depth and colorimetric measurements at the surface performed in New Zealand geothermal areas. Since the method is empiric and strongly affected by the soil properties it is not easily applicable to other areas. Furthermore Fridriksson et al (2006), who performed a comparison between the Dawson (1964) method and that based on the CO₂ flux (i.e. the same we applied at Copahue) found a difference of about one order of magnitude and concluded: *“The discrepancy between the observed heat loss and the heat loss inferred from the CO₂ emissions is attributed to steam condensation in the subsurface due to interactions with cold ground water. **These results demonstrate that soil diffuse degassing can be a more reliable proxy for heat loss from geothermal systems than soil temperatures.**”*

For these reasons we did not apply the method based on soil temperature measurements but we qualitatively discuss the spatial correlations between CO₂ flux and soil temperatures.

2) Evaluation of potential future geothermal power production

In our work we gave a detailed picture of the natural heat flux from the surveyed areas and this was one of the aims of our work. For instance, typically the energy conversion efficiency from thermal energy to electric is 0.1 (so the estimated heat release of 110 MW would return 11 MW, but this is a minimum estimation because most of the geothermal power plants exploit the thermal energy 'stored' in the fields and not just the natural flux). However we don't want enter in this topic because the eventual future geothermal power production will depend on many other engineering and political factors.

3) Carbon isotopic composition of CO₂ efflux.

In the text we discussed this point highlighting that a better definition of the CO₂ sources would have been done with the availability of isotopic data. The measurements were not performed mainly for logistical problems because the samples have to be analyzed in a short

Instituto de Estudios Andinos Don Pablo Groeber

Departamento de Geología – Facultad de Ciencias Exactas y Naturales
Universidad de Buenos Aires

Pabellón II – Entrepiso – Oficina 29

Ciudad Universitaria (1428) Buenos Aires

+54 11 4576 3400

idean@gl.fcen.uba.ar

<http://www.idean.gl.fcen.uba.ar>



time (typically in a week) and this was impossible. As described in the text we used other methods to discriminate between background and hydrothermal-volcanic CO₂ sources.

We followed most of the minor suggestions in the text, including Fig. 3 that was re-drawn to better highlight the measuring point location

Reviewer#2

This is a nice paper that quantifies CO₂ and heat emissions from hydrothermal systems associated with the Copahue-Caviahue volcanic complex, Argentina. CO₂ emissions were directly measured and heat emissions were inferred using CO₂ as a tracer of the original vapor phase. The paper serves as a contribution to the global inventory on volcanic-hydrothermal CO₂ emissions and, more locally, provides better understanding of the geothermal potential of the volcanic complex. Only minor changes are suggested.

Thank you

Specific comments:

1) I suggest changing "Copahue volcano" in the paper title to "the Copahue-Caviahue volcanic complex" to broaden the study site out.

Done.

2) Line 42: change "80's" to "1980's".

Done.

3) Line 44 and elsewhere throughout the text: I think "unique vapor zone" would be better described as a single vapor zone, i.e., "...indicate the presence of a single large vapor zone at 200-2100..."

We maintain the term 'unique' because it refers to the existence of only one large vapor zone feeding the degassing process. This, as explained in the text, is strongly suggested by the compositional homogeneity of the fumaroles collected from the different investigated sites.

4) Line 48 and elsewhere throughout the text: "large extension of the hydrothermal areas" would be better expressed as "wide expanse of..." or "wide spatial distribution of..."

Done.

5) The following parts of the Materials and methods section (3) belonging in the Results section: (1) lines 165-168; (2) Table1; (3) lines 203-205; (4) Table 2; Line 223; Line 248; (5)

Instituto de Estudios Andinos Don Pablo Groeber

Departamento de Geología – Facultad de Ciencias Exactas y Naturales
Universidad de Buenos Aires
Pabellón II – Entrepiso – Oficina 29
Ciudad Universitaria (1428) Buenos Aires
+54 11 4576 3400
idean@gl.fcen.uba.ar
<http://www.idean.gl.fcen.uba.ar>



Table 3; (6) Table 4; (7) Lines 285-287.

We partly followed this suggestion: Table 1 and 2, where the analytical data and survey parameters are reported, were included in the material and methods section, while Table 3 and 4, where interpretative results are reported, were moved in the results section.

6) Throughout the Materials and Methods section, there seems to be quite a lot of descriptive text devoted to well-established methods that are already presented in the literature and could probably be cut from here. For example, could just Lines 181-183 be kept and Lines 184-201 be eliminated? Other methods descriptions could be trimmed as well.

We respectfully disagree with the reviewer because in our work we used instruments that were developed and set up in our laboratories. Those sentences are meant to describe the peculiar characteristics of these not-commercial instruments, which we think are of interest for the readers.

7) For consistency, I suggest moving subsection 3.3 up to 3.2 (after fumarole chemistry).

Done.

8) Figure 5 and page 18, paragraph 2: I find it rather difficult to see some of the spatial trends described in this paragraph in the soil CO₂ flux maps. In some cases, I see linear features in the soil CO₂ flux distributions, but in others, only round-ish blobs. Are all of the inferred faults on Figure 5 inferred based on the soil CO₂ flux maps, or are some of them inferred based on previous geologic/structural studies? Please clarify. Also, I suggest loosening the language when describing the DDS geometries and their relationship to structural trends. For example, in Line 419: "...are roughly consistent..." Line 423: "...roughly develop along..." **In our opinion the general structural control on diffuse degassing is quite evident (in particular in the largest surveyed areas, i.e. Termas de Copahue and Las Machinas). However we followed the reviewer suggestion and we 'loosen' the language.**

9) Figure 5: Because the grey stripes showing the extent of the "hot area" do not overlap on Termas de Copahue and Las Maquinas, it looks like these thermal areas are not located within this area. An outline around the hot area might show its extent more clearly.

Done.

10) Lines 432-434 and Lines 408-411: I would suggest stating early on in the Results section (when you move Table 1 to the Results and first describe it there) the observations that the compositions of fumaroles at Termas de Copahue, Las Maquinas, and Las Maquinas II are very similar, while Anfiteatro is different.

We did not move Table 1 and we think that the comment about the strong similarity among fumarole compositions is more incisive in this part of the text. Also in order to avoid repetitions we did not move these observations.



11) Lines 472-477: Confusing- rewrite more clearly.

For typing error the same observation was repeated in 2 sentences. We corrected this error and we think that now the sentence is clearer.

12) Line 499: Change "subsoil" to "subsurface".

Done.

Once again, thank you very much for your time and assistance.

Best Regards,

Lic. María Clara Lamberti

Corresponding author

E-mail: mclamberti@gl.fcen.uba.ar

Highlights

- We mapped and quantified deeply derived CO₂ diffuse flux at Caviahue caldera
- About 165 t/d of CO₂ is released as diffuse degassing.
- The degassing is related to a geothermal reservoir containing a single vapor phase
- We computed a natural thermal release of 107 MW
- An active magmatic intrusion beneath the studied portion of the Caviahue caldera is suggested

1 **CARBON DIOXIDE DIFFUSE EMISSION AND THERMAL ENERGY RELEASE**
2 **FROM HYDROTHERMAL SYSTEMS AT COPAHUE-CAVIAHUE VOLCANIC**
3 **COMPLEX (ARGENTINA)**

4

5 Giovanni Chiodini¹, Carlo Cardellini², María Clara Lamberti^{3*}, Mariano Augusto³, Alberto
6 Caselli⁴, Caterina Liccioli³, Giancarlo Tamburello⁵, Franco Tassi^{6,7}, Orlando Vaselli^{6,7},
7 Stefano Caliro⁸

8

9 1. Istituto Nazionale di Geofisica e Vulcanologia, Sezione di Bologna, Via D. Creti 12, 40128
10 Bologna, Italy.

11 2. Università degli Studi di Perugia, Dipartimento di Fisica e Geologia, Via G. Pascoli snc, I-06123
12 Perugia, Italy.

13 3. IDEAN-GESVA, Dpto. Cs. Geológicas, FCEN, Universidad de Buenos Aires, Buenos Aires,
14 Argentina.

15 4. LESVA-IIPG. Universidad Nacional de Río Negro, General Roca, Argentina.

16 5. Università degli Studi di Palermo, DiSTeM, Via Archirafi 36, I-90123 Palermo, Italy.

17 6. Università degli Studi di Firenze, Dipartimento di Scienze della Terra, Via G La Pira 4, I-50121
18 Firenze, Italy.

19 7. Istituto di Geoscienze e Georisorse – Consiglio Nazionale delle Ricerche (CNR-IGG), Via La
20 Pira, 4, I-50121, Firenze, Italy.

21 8. Istituto Nazionale di Geofisica e Vulcanologia, Sezione di Napoli - Osservatorio Vesuviano, Via
22 Diocleziano 328, I-80124 Napoli, Italy.

23

24 *corresponding author: mclamberti@gl.fcen.uba.ar; Tel: + 54 114576 3400

25

26

27 **Highlights**

- 28 • We mapped and quantified deeply derived CO₂ diffuse flux at Caviahue caldera
29 • About 165 t/d of CO₂ is released as diffuse degassing.
30 • The degassing is related to a geothermal reservoir containing a single vapor phase
31 • We computed a natural thermal release of 107 MW
32 • An active magmatic intrusion beneath the studied portion of the Caviahue caldera is
33 suggested

34 **Abstract**

35 The north-western sector of Caviahue caldera (Argentina), close to the active volcanic
36 system of Copahue, is characterized by the presence of several hydrothermal sites that host
37 numerous fumarolic emissions, anomalous soil diffuse degassing of CO₂ and hot soils. In
38 March 2014, measurements of soil CO₂ fluxes in 5 of these sites (namely, Las Máquinas,
39 Las Maquinitas I, Las Maquinitas II, Anfiteatro, and Termas de Copahue) allowed to
40 estimate that ~165 tons of deeply derived CO₂ are daily released. The gas source is likely
41 related to a relatively shallow geothermal reservoir containing a single vapor phase as also
42 suggested by both the geochemical data from the 3 deep wells drilled in the 1980's and gas
43 geoindicators applied to the fumarolic discharges. Gas equilibria within the H-C-O gas
44 system indicate the presence of a large, probably unique, single phase vapor zone at 200-
45 210 °C feeding the hydrothermal manifestations of Las Máquinas, Las Maquinitas I and II
46 and Termas de Copahue. A natural thermal release of 107 MW was computed by using CO₂
47 as a tracer of the original vapor phase. The magmatic signature of the incondensable
48 fumarolic gases, the wide expanse of the hydrothermal areas and the remarkable high
49 amount of gas and heat released by fluid expulsion seem to be compatible with an active
50 magmatic intrusion beneath this portion of the Caviahue caldera.

51

52

53 **1. Introduction**

54 The poor knowledge of CO₂ fluxes released from natural sources, such as mantle
55 and metamorphic reactions, is one of the most vexing problems in understanding the
56 geological carbon cycle (Berner and Lagasa 1989). Large uncertainties affect the estimates
57 of global CO₂ flux from volcanoes (Burton et al. 2013 and reference therein) due to the
58 relatively limited flux measurements of volcanic plumes from persistently degassing
59 volcanoes. In addition, the amount of CO₂ not directly related to volcanic craters and
60 released from hydrothermal systems associated with most active volcanic regions is poorly
61 constrained. Recently, an international initiative to fill this gap has been promoted by the
62 scientific community with a project named DECADE ([https://deepcarbon.net/content/deep-
63 carbon-observatory-launches-decade-initiative](https://deepcarbon.net/content/deep-carbon-observatory-launches-decade-initiative)), which supports investigations focused on
64 the study of CO₂ fluxes from active volcanoes. The present study is in the framework of

65 this initiative, being aimed at mapping and quantifying deep-originated CO₂, diffusively
66 discharged from the hydrothermal areas located few kilometers east of the active volcanic
67 system of Copahue (Patagonia, Argentina), where fumarolic discharges and large zones of
68 soil diffuse gas emission occur. A second goal of this study is that to provide an estimation
69 of the local geothermal potential.

70 The development of a quick and reliable technique for the measurements of soil
71 CO₂ fluxes (Chiodini et al. 1998) has recently promoted applications in different fields of
72 geological and environmental sciences. One of the most promising applications of this tool
73 (namely, the accumulation chamber method) regards the use of soil CO₂ flux surveys for
74 geothermal prospecting. This method allows to recognize and characterize CO₂ flux
75 anomalies at the surface, which are caused by the circulation of hydrothermal fluids at
76 depth. Soil CO₂ fluxes higher than those due to biologic activity are indeed commonly
77 associated with the circulation of hydrothermal fluids (Chiodini et al. 1998; Cardellini et al.
78 2003; Lewicki and Oldenburg 2005). In addition, recent studies have shown that CO₂
79 diffuse degassing can provide important and reliable constraints for a correct evaluation of
80 the geothermal potential from hydrothermal areas (Chiodini et al. 2005; Fridriksson et al.
81 2006; Werner and Cardellini 2006; Chiodini et al. 2007; Mazot and Taran 2009; Hernández
82 et al. 2012; Rissmann et al. 2012; Bloomberg et al. 2014; Granieri et al. 2014; Dionis et al.
83 2015). In particular, the total budget of hydrothermal gases released at the surface can be
84 used for a robust estimation of the minimum amount of geothermal fluids involved at depth
85 in the degassing process. Consequently, the accumulation chamber method represents an
86 effective, rapid and cheap instrumentation for estimating the minimum geothermal potential
87 of an unknown area since the thermal energy naturally transported and released by the
88 fluids can be evaluated.

89

90 **2. Geological, volcanological and hydrothermal setting**

91 The Copahue-Caviahue Volcanic Complex (hereafter CCVC, 38°S-71°W) is
92 located in the Neuquén Province (Patagonia, Argentina) on a segment of the Andes range,
93 called the South Volcanic Zone (hereafter SVZ: 33.3° - 46°S), 30 km east of the main
94 Pleistocene-Holocene volcanic front (Fig. 1). Volcanism in the SVZ is related to the

95 subduction of the Nazca Plate beneath the South American Plate, at rates as high as 10.8 cm
96 y^{-1} (DeMets et al. 1994; Ramos and Folguera 2000; Melnick et al. 2006).

97

98 **Figure 1.** a) Geological, volcanological and structural setting of the Copahue-Caviahue Volcanic Complex
99 and location of the study area (modified from Folguera et al. 2004); b) location of the surveyed hydrothermal
100 sites.

101

102 The steepening of the oceanic plate subducted in the last 5 Ma resulted in the displacement
103 of the asthenospheric wedge and an asthenospheric upwelling. This process favored a process
104 of crustal thinning that caused the most recent westward migration of the volcanic arc,
105 extensional dynamics and large effusions of basaltic-andesitic magma (Folguera et al. 2006;
106 Yuan et al. 2006).

107 The CCVC includes the Caviahue Caldera (also known as Caldera del Agrio), a
108 volcano-tectonic depression defined as an intra-arc extensional pull-apart basin (Ramos and
109 Folguera 2000; Bermúdez et al. 2002; Melnick et al. 2006; Rojas Vera et al. 2010). The
110 pull-apart basin is located at the transition zone between the Liquiñe-Ofqui dextral-slip and
111 the Antañir-Copahue fault systems (Lavenu and Cembraro 1999, Folguera et al. 2004). The
112 former accommodates lateral displacements imposed by the oblique convergence between
113 the Nazca and South American plates from $\sim 46^{\circ}\text{S}$ to $\sim 38^{\circ}\text{S}$ (Radic 2010). The CCVC
114 encompasses the Copahue volcano, a Pleistocene polygenic stratovolcano located in the
115 southwestern rim of the Caviahue Caldera, whose main products are andesites and basalts
116 (Polanco 2003). The easternmost of the nine NE-oriented summit craters of the Copahue
117 volcano is currently active. During the last 250 years, at least thirteen low-magnitude
118 phreatic and phreatomagmatic eruptions occurred from this crater (Martini et al. 1997;
119 Naranjo and Polanco 2004). The 1992 and 1995 eruptions mostly consisted of phreatic
120 events characterized by the emission of pyroclastic sulfur. In 2000, a phreatomagmatic
121 eruption, mainly involving juvenile material, occurred (Delpino and Bermúdez 1993; 2002;
122 GVN 2000a; 2000b). Since November-December 2011, the discharge rate of fluids from
123 the Copahue active crater increased, whereas sporadic phreatic events **have** been occurring
124 since July 2012. A major phreatomagmatic-magmatic eruption was observed on December
125 22, 2012 **and a significant degassing** is still ongoing (Caselli et al. 2015).

126 During quiescent periods, the active crater hosts a hot acidic lake (up to 63 °C and
127 pH<1) (Varekamp et al. 2001; 2009; Agosto 2011; Agosto et al. 2012; 2013). Two acidic
128 hot springs (up to 80 °C and pH = 1-2) discharge in the eastern summit flank of the cone
129 and merge downstream to form the upper Agrio river (pH = 2-3), which flows into the
130 acidified glacial Lake Caviahue (Martini et al. 1997; Gammons et al. 2005; Varekamp et al.
131 2008; Caselli et al. 2005; Agosto 2011; Agosto and Varekamp 2015).

132 In March 2014, a remote sensing campaign, carried out by combining MiniDoas and
133 Multigas techniques, revealed the presence of an important gas plume from the crater lake
134 and allowed a rough estimation of the released SO₂ and CO₂, which resulted to be of ~960
135 and ~640 ton d⁻¹, respectively (Tamburello et al., 2015).

136 In the north-eastern flank of the Copahue volcanic edifice, within the Caviahue
137 Caldera, six hydrothermal areas **are** recognized: Las Máquinas, Las Maquinitas I, Las
138 Maquinitas II, Anfiteatro, Termas de Copahue and Chanco-Co (Mas et al. 1996; 2000;
139 Fig. 1). The hydrothermal activity of some of these sites (Las Máquinas, Las Maquinitas
140 and Termas de Copahue) is so intense **that causes** a background volcanic tremor as revealed
141 by a seismic array analysis performed in the 2003-2005 period (Ibañez et al. 2008). Fluids
142 are discharged as boiling, bubbling and mud pools (up to temperatures of 96 °C), fumaroles
143 (up to 130 °C at La Maquinitas I) and larges areas of diffuse degassing and hot soils.
144 According to the recent, comprehensive study of the hydrothermal-volcanic fluids at CCVC
145 by Agosto et al. (2013), the fumarole chemistry suggested that the gas source was
146 associated with boiling processes of a hydrothermal system, mainly fed by meteoric water,
147 although affected by magmatic fluids of mantle signature, as indicated by the relatively
148 high ³He/⁴He ratios (R/Ra >7).

149

150 **3. Material and methods**

151 **3.1 Sampling and analysis of gas from fumaroles**

152 Fumarolic discharges from the thermal areas of Las Máquinas, Las Maquinitas I and
153 II, Termas de Copahue and Anfiteatro were collected in March 2012 by using pre-
154 evacuated flasks containing a 4N NaOH solution (Giggenbach 1975; Giggenbach and
155 Gouguel 1989) for the analysis of the major gas species. Vapor condensates and, separately,
156 dry gases were sampled using a condenser, cooled at ~20–30 °C by cold water. The

157 chemical analyses were carried out at Osservatorio Vesuviano (INGV) laboratories. The
158 gas chemistry of non-absorbed gases, present in the headspace over the NaOH solution,
159 was **determined** by gas chromatography through a unique injection on two molecular sieve
160 columns (MS 5 Å capillary, 30 m × 0.53 mm × 50 µm; He and Ar as carrier gases) using
161 TCD detectors. Carbon dioxide and sulfur species absorbed in the alkaline solution were
162 analyzed after oxidation via H₂O₂, by acid–base titration and ion chromatography,
163 respectively (analytical error ±3%). Because of reaction in alkaline solution to form COOH⁻
164 (Giggenbach and Matsuo 1991), CO was analyzed **on dry** gas samples by gas
165 chromatographic separation with a MS 5 Å 1/8 × 50 in column (He as carrier gas) coupled
166 with a high-sensitivity Reduced Gas Detector (HgO). The analytical results are reported in
167 Table 1. In the Table 1 the ³He/⁴He isotopic ratios, expressed as R/Ra where R is the
168 measured ³He/⁴He ratio and Ra is that of air (1.39×10⁻⁶), **are from** Augusto et al. (2013).

169

170 **Table 1. Chemical composition** of the fumaroles of the surveyed areas (March 2012). Gas concentrations are
171 expressed in µmol/mol, helium isotopes as R/Ra (³He/⁴He_{sample}/³He/⁴He_{air}). **Equilibrium temperatures were**
172 **calculated within the H₂O-H₂-CO₂-CO-CH₄ gas system (T_{H-C-O}; Tassi et al., 2015) and the geothermometer**
173 **based on the CO/CO₂ ratio (T_{CO-CO2}; Chiodini et al., 2015).**

174

175

176

3.2 Fumarolic flux

177 **A well defined gas plume, suitable for the determination of the CO₂ flux discharged**
178 **by the fumarolic vent, was found at Las Maquinitas I. Here, the technique proposed by**
179 **Aiuppa et al. (2013) was applied.** The method consists on the measurement of the
180 **Integrated Column Amount** (ICA, kg m⁻¹) of CO₂ that is subsequently multiplied by the
181 plume transport speed (m/s) to calculate the flux. **The concentration in the plume of CO₂, as**
182 **well as that of other gases (not discussed here), was** measured with a portable MultiGAS
183 system (Aiuppa et al. 2013 and references therein) along the horizontal and vertical axes of
184 an orthogonal **cross-section** of the plume. During the measurements the plume was sub-
185 **horizontal as the wind was blowing to the East** with constant speed. We calculated the
186 average CO₂ concentration of ~90 samples (0.5 Hz sampling rate) every meter on **an 8 m**
187 long horizontal **axis**, and every 0.4 m on a 2.4 m **high vertical axis**. The gas velocity was
188 determined by tracking the transport speeds of individual gas puffs on a **video recorder** with

189 a Nikon D90 video camera. The measured plume speed of $6.9 \pm 2.2 \text{ m s}^{-1}$ leads to a CO_2
190 flux of $3.2 \pm 1.1 \text{ t d}^{-1}$.

191

192

193 **3.3 Soil CO_2 flux and temperatures**

194 Soil CO_2 flux (ϕCO_2) and temperatures (1,763 measurements) were measured at Las
195 Máquinas, Las Maquinitas I and II, Anfiteatro, and Termas de Copahue (total investigated
196 area = 1.21 km^2 ; Fig. 1b). The degassing area of Chanco-Co was not investigated due to
197 logistical problems.

198 Soil CO_2 fluxes (ϕCO_2) were measured using two accumulation chamber devices
199 developed and calibrated at the laboratories of Osservatorio Vesuviano and University of
200 Perugia. The two equipments, operating in a dynamic mode as described in Chiodini et al.
201 (1998), consist of: 1) a metal cylindrical vessel (the chamber, AC), 2) an Infra-Red (IR)
202 spectrophotometer, 3) an analog-digital (AD) converter, and 4) a palmtop computer. The
203 AC has a volume of $\sim 2.8 \text{ L}$ and is equipped with a ring-shaped perforated manifold re-
204 injecting the circulating gas to ensure the mixing of the air in the chamber. The IR
205 spectrometers consist of LICOR Li-800 and LICOR Li-820 detectors equipped with sensors
206 operating in the range 0-20,000 ppm of CO_2 . The soil gas circulates from the chamber to
207 the IR sensor and vice versa by a pump ($\sim 1 \text{ L min}^{-1}$). The CO_2 concentration inside the AC
208 is acquired every 250 msec. The signal is converted by the AD and transmitted to a palmtop
209 computer, where a CO_2 concentration vs. time diagram is plotted in a real time. The ϕCO_2
210 is computed from the rate of CO_2 concentration increase in the chamber (dC_{CO_2}/dt),
211 according to the following equation:

212

$$213 \quad \phi\text{CO}_2 = cf \times dC_{\text{CO}_2}/dt. \quad (1)$$

214

215 The proportionality factor (cf) between dC_{CO_2}/dt and ϕCO_2 was determined before
216 the survey during laboratory tests. The ϕCO_2 values, typically from 10 to $10,000 \text{ g m}^{-2} \text{ d}^{-1}$,
217 were measured on a “synthetic soil” made of dry sand (10 cm thick) placed inside a plastic

218 box with an open top. The cf factor was then computed as **the slope of the linear best-fit**
219 **ϕCO_2 vs. $d\text{C}_{\text{CO}_2}/dt$ straight line.**

220 Soil temperature was measured at the depth of 10 **cm by means of** a thermocouple
221 equipped with a metallic probe.

222 The extension of the **five** surveyed areas, together with the number and the range of
223 the **CO_2 flux (ϕCO_2) measurements for each area**, are reported in Table 2. The complete set
224 **of the ϕCO_2 data is available** in the supplementary material (SM1).

225

226 **Table 2.** Main parameters **of the five** surveyed areas.

227

228 **3.4 Soil CO_2 fluxes and temperatures data processing**

229 The ϕCO_2 data were **used** to compute the total CO_2 release from the deep volcanic-
230 hydrothermal source and to map its spatial distribution, **as well as** that of the soil
231 temperature, by applying the Graphical statistical approach (GSA) and the sequential
232 Gaussian simulations (SGS) methods.

233 Soil CO_2 flux values in hydrothermal areas are characterized by complex statistical
234 distributions, which generally reflect the coexistence of different CO_2 sources such as
235 biogenic and endogenous (Cardellini et al. 2003). In a logarithmic probability plot, where a
236 straight line describes one log-normal population, these complex distributions result on a
237 curve with n inflection points, which describes the overlapping of $n+1$ log-normal
238 populations.

239 The GSA method (Chiodini et al. 1998) was used to both partitioning these
240 distributions into the individual log-normal populations and estimating their proportion (f_i),
241 mean value and standard deviation. The partition was performed according to the graphical
242 procedure proposed by Sinclair (1974). Since the computed statistical parameters of the
243 populations (i.e. mean and standard deviation) refer to the logarithm of values, the mean
244 value of ϕCO_2 (M_i) and the central 90% confidence interval of the mean were estimated by
245 means of a Montecarlo procedure. The estimated mean flux values were used to compute
246 the CO_2 released from the investigated areas and associated with each population by
247 multiplying M_i by the respective covered surface (S_i), the latter being assumed as a fraction
248 of the total surveyed area (S), which corresponds to the relative proportion of the

249 population (i.e. $S_i = f_i \times S$). The total CO₂ release from the entire area can then be obtained
250 by summing up the contribution of each population (i.e. $\sum f_i \times M_i \times S$). Similarly, the central
251 90% confidence interval of the mean value was used to calculate the uncertainty of the total
252 CO₂ output estimation of each population.

253 Although the GSA approach is a useful tool for the interpretation of the diffuse
254 degassing process, the results obtained by this method can be affected by some arbitrary
255 choices, as follows: i) the polymodal log-normal distribution of CO₂ flux values is a
256 convenient model for subsequent partitioning. Nevertheless, the statistical distribution of
257 the CO₂ flux can be more complex than that of a simple log-normal distribution, ii) the
258 partitioning procedure does not imply a unique solution, iii) the spatial distribution of the
259 measured values is not considered by this statistical approach, and iv) the interpretations of
260 the CO₂ flux distribution at the tails, especially for high flux values, can highly be affected
261 by a low number of measured values. As a consequence of the latter “choice”, the estimate
262 of the total CO₂ output can be subjected to remarkable differences.

263 An alternative and more reliable estimation of the total CO₂ output **can be obtained**
264 **from the** CO₂ flux mapping **by** the Sequential Gaussian Simulation (SGS) algorithm
265 provided by the sgsim code (Deutsch and Journel 1998). According to Cardellini et al.
266 (2003) and Lewicki et al. (2005), SGS yields a realistic representation of the spatial
267 distribution of the CO₂ fluxes reproducing the histogram and variogram of the original data.

268 The SGS method produces numerous equiprobable and alternative simulations of the
269 spatial distribution of the attribute, i.e. CO₂ flux and temperature in this work. Since the
270 SGS procedure requires a multi-Gaussian distribution, original data were transformed into
271 normal distribution by a normal score transform (Deutsch and Journel 1998; Cardellini et
272 al. 2003). Experimental variograms of the normal scores were computed and modeled for
273 each data set. The models were used in the SGS procedure to create 200 simulations of the
274 normal scores. The simulated normal scores were then **back-transformed** into values
275 expressed in original data units, applying the inverse of the normal score transform. **The**
276 **average of the values simulated at each cell of the grid in the 200 simulations were used to**
277 **draw the maps of soil CO₂ flux and soil temperature. For each simulation the total CO₂**
278 **release was computed by summing up the products of the simulated value of each grid cell**
279 **by the cell surface. The mean and the standard deviation of the 200 values of total CO₂**

280 output were assumed to be the characteristic values of the CO₂ release and of its
281 uncertainty, respectively, for each surveyed area.

282

283 4. Results and discussions

284 4.1 CO₂ soil degassing

285 The investigated areas were characterized by a wide range of CO₂ flux values,
286 which varied from <0.05 g m⁻² d⁻¹ to >16,560 g m⁻² d⁻¹ (Table. 2). Each data set is reported
287 in the logarithmic probability plots of Figure 2. These diagrams show the results of the
288 GSA analysis, which includes i) the partitioned log-normal populations (blue straight lines),
289 ii) their proportion, mean and standard deviation, and iii) the theoretical statistical
290 distribution resulting from the combinations of the individual populations (red dashed
291 curves).

292 The proportion, mean and standard deviation and the total CO₂ output calculated for
293 each population are reported in Table 3.

294

295 **Figure 2.** Probability plots of Log ϕ CO₂ for the different hydrothermal sites and partition of the distributions
296 in log-normal populations (blue lines).

297

298 **Table 3.** Estimated parameters and partitioned populations in the 5 surveyed areas.

299

300 On the basis of the mean flux values characterizing the different populations, an
301 interpretation of the main CO₂ source is reported in Table 3. “Background” refers to CO₂
302 fluxes related to soil respiration, whereas the term “endogenous” is related to those fluxes
303 fed by volcanic-hydrothermal degassing. The latter includes those populations
304 characterized by high mean ϕ CO₂ values, typically in the order of 10³ g m⁻²d⁻¹, i.e. much
305 higher than those produced by biogenic sources in the soil, which typically are 2-3 order of
306 magnitude lower (e.g., Raich and Schlesinger 1992; Raich and Tufekcioglu 2000;
307 Cardellini et al. 2003). At Las Máquinas, Anfiteatro and Termas de Copahue, the
308 distribution of the CO₂ flux values in the probability plots indicates the presence of more
309 than one “background” population (Table 3). The occurrence of different background
310 populations possibly reflects the presence of different soils and vegetation in the surveyed
311 areas. The background populations with the lowest mean values of ϕ CO₂ (normally <1 g m⁻²

312 $^2\text{d}^{-1}$) correspond to fluxes from bare altered soils. Such low values could nevertheless be
313 referred to an endogenous source, although their origin cannot properly be assessed since
314 no isotopic carbon values of the CO_2 efflux (Chiodini et al., 2008) are available. However,
315 it is to be pointed out that contributions by low flux populations to the total CO_2 budget are
316 negligible. The relatively high ϕCO_2 values, which characterize the background populations
317 “B” at Las Máquinas ($24 \text{ g m}^{-2}\text{d}^{-1}$), C at Anfiteatro ($26 \text{ g m}^{-2}\text{d}^{-1}$), and B at Termas de
318 Copahue ($22 \text{ g m}^{-2}\text{d}^{-1}$), are mainly representative of the presence in the surveyed areas of
319 wet soils and peat (Table 3).

320 The estimated total CO_2 outputs using the GSA approach, i.e. the sum of all
321 contributions from the different populations, range from 4.4 t d^{-1} (Las Maquinitas I) to 119 t
322 d^{-1} (Termas de Copahue). The central 90% confidence interval of the mean value is
323 generally large and, especially at Anfiteatro and Las Maquinitas II, it varies of one order of
324 magnitude ($11\text{-}110 \text{ t d}^{-1}$ and $4\text{-}44 \text{ t d}^{-1}$, respectively). These large uncertainties mainly
325 depend on the relatively low number of samples available for the definition of the high-flux
326 populations, which mostly contribute to the total CO_2 output. On the contrary, the
327 computations of the background populations are affected by a lower uncertainty because
328 they are less variable and are defined by numerous samples (Fig. 2, Table 3). Assuming that
329 CO_2 of the background populations is totally derived from shallow biogenic sources (soil
330 respiration, e.g. Raich and Schlesinger 1992), the total background CO_2 output is of 5.9 t d^{-1}
331 at Las Máquinas, nil at Las Maquinitas I, 0.09 t d^{-1} at Las Maquinitas II, 3.3 t d^{-1} at
332 Anfiteatro and 9.2 t d^{-1} at Termas de Copahue.

333 In order to map the CO_2 fluxes and to compute the total gas release using the SGS
334 approach, experimental variograms of the normal scores of the data were computed and
335 modeled for each data set (Table 4). The models were used in the SGS procedure to create
336 200 simulations of the CO_2 flux according to the computation grids described in Table 4.
337 The obtained CO_2 flux maps are reported in Figure 3.

338

339

340

341

342

343

344

345 **Table 4.** Relevant parameters of SGS application and estimation of the total CO₂ output from Copahue
346 hydrothermal sites.

347

348 All the surveyed areas are characterized by a well-defined Diffuse Degassing
349 Structure (DDS), except at Anfiteatro where the CO₂ fluxes are less spatially organized.

350

351 **Figure 3.** Maps of the CO₂ flux for the different hydrothermal sites (map coordinates are expressed in m,
352 UTM-WGS84 19S).

353

354 The total SGS-computed CO₂ release ranged from 5 t d⁻¹ (Las Maquinitas I) to 100 t
355 d⁻¹ (Termas de Copahue) with a relatively low uncertainty (≤10%; Table 4). These values
356 can be considered comparable with those obtained by the GSA approach, except for Las
357 Maquinitas II and Anfiteatro, where the SGS estimates are about 50% less than those
358 obtained by GSA. These differences are likely related to an overestimation computed by
359 GSA because a relatively low number of CO₂ flux measurements are available for the
360 definition of the high flux populations. For this reason, the total CO₂ release obtained by
361 the SGS approach was preferred for further computations.

362 The amount of released endogenous CO₂ (Q_{CO2}) was computed for each area by
363 subtracting the specific background contribution estimated by GSA to the total CO₂ release
364 estimated by SGS. The computed Q_{CO2} varies from 5 t d⁻¹ (Las Maquinitas I) to 90.8 t d⁻¹
365 (Termas de Copahue) (Table 4).

366

367 **4.2 Soil temperature distribution**

368 The soil temperature maps obtained by applying the SGS algorithm are reported in
369 Figure 4 and refer to the temperature at 10 cm depth, concurrently measured with each
370 φCO₂ measurement.

371 Setting aside Anfiteatro, the soil temperature spatial distribution (Fig. 4) in the
372 investigated areas closely mimics that of φCO₂ (Fig. 3). A correlation between soil
373 temperature and φCO₂ is not surprising because the presence of fumarolic emission favors a
374 massive steam condensation at shallow depth, heating the soil by the latent heat of

375 condensation and causing a flux of incondensable gases (i.e. mostly CO₂) toward the
376 surface (Chiodini et al. 2001; 2005). Accordingly, in areas of fumarolic discharges, hot
377 soils and anomalous diffuse soil degassing of incondensable gases, CO₂ flux can be used as
378 a tracer of the whole process allowing to estimate the total amount of steam and thermal
379 energy involved in the process.

380

381 **Figure 4.** Maps of soil temperature for the different hydrothermal sites (map coordinates are expressed, in m
382 UTM-WGS84 19S).

383

384 **4.3 The hydrothermal system feeding soil diffuse degassing and structural** 385 **control on DDS**

386 The main fumarolic emissions located in the five surveyed zones (Figs. 1 - 4) were
387 sampled and analyzed in 2012. The concentration of main and relevant gas species, C and
388 He isotopes and the temperature estimations calculated by gas geothermometry are reported
389 in Table 1. H₂O is by far the main component, being > 97% by volume in all the fumaroles.
390 The second component is CO₂, followed by minor amount of N₂, H₂, CH₄ and H₂S. CO and
391 He concentrations are <1 ppm by volume. The absence of the strong acidic gases (i.e. SO₂,
392 HCl and HF), which are typical of high temperature fumaroles from active volcanic
393 systems, and the relatively high CH₄ contents suggest that these gases are intimately related
394 to a hydrothermal system. According to Agosto et al. (2013), the fumarolic fluids are
395 originated by boiling of a hydrothermal reservoir, mainly fed by meteoric water. However,
396 the high ³He/⁴He ratios (R/Ra up to 7.04), the δ¹³C-CO₂ values of ~ -7‰ and the N₂/Ar
397 ratios much higher than those of ASW (**Air Saturated Water**), suggest that He, N₂ and CO₂
398 are mainly supplied to the hydrothermal system by a magmatic source (Agosto et al. 2013;
399 Tassi et al. 2015). Three deep wells, drilled in the eighties in the frame of a geothermal
400 project (COP-1, COP-2 and COP-3 in Fig. 5; Dellapé and Pando 1975; Jurío 1977;
401 Panarello et al. 1988; JICA-EPEN 1992; Sierra et al. 1992; Mas et al. 2000), provided
402 direct information on the hydrothermal system feeding the CCVC diffuse degassing
403 structures. All the 3 wells, which are located 1-2 km S or W of the studied hydrothermal
404 sites (Fig. 5), reached a deep reservoir of high temperatures (240-260 °C) and a shallower
405 vapor dominated zone at depths of 800-1,000 m for which temperatures from 200 to 215 °C

406 were measured and/or estimated with geochemical indicators (Sierra et al. 1990; Panarello
407 2002).

408

409 **Figure 5.** Structural setting for area compared with the location of DDSs and geothermal wells. The area
410 where we infer the presence at depth of a single phase vapor zone is highlighted.

411

412 Geothermometric calculations in the H₂O-CO₂-CH₄-CO-H₂ gas system (Tassi et al. 2015)
413 indicated that the fumarolic fluids discharged at Piedra Copahue, Las Máquinas and Las
414 Maquinitas equilibrate in a single vapor phase, as actually observed by the geothermal
415 wells, at a temperature of 203-210 °C (T_{H-C-O} in Table 1). Other computations, based on the
416 CO/CO₂ ratios by applying the same method described in Chiodini et al. (2015), produced
417 similar temperatures (T_{CO-CO₂} ~204-206 °C; Table 1). These estimations are in good
418 agreement with the temperatures measured in the geothermal wells, suggesting the
419 occurrence of a large, probably unique, vapor zone reached by the wells and feeding the
420 hydrothermal manifestations of Termas de Copahue, Las Máquinas and Las Maquinitas
421 (“hot area with evidences of a single phase vapor zone **at depth**” in Fig. 5). This would
422 explain the remarkable chemical and isotopic homogeneity of the fumaroles from the 3
423 different sites (Table 1), which are distant a few kilometers from each other (Fig. 5). The
424 three fumaroles show, for example, a similar H₂O/CO₂ molar ratio of ~40 and ³He/⁴He of
425 ~7 R/Ra.

426 In order to better understand the role of this vapor zone in the hydrothermal
427 circulation, the structural setting of the zone **needs** to be considered. The caldera is locally
428 characterized by three fault systems, which are NE-SW, WNW-ESE and NW-SE oriented
429 (Melnick et al. 2006; Rojas Vera et al. 2010; Latinoconsult 1981; JICA – EPEN 1992).
430 These three fault systems are arranged in such a way that they constitute the borders of a
431 triangle-shaped horst structure which, according to gravity and electrical resistivity surveys,
432 represents a high conductivity zone of hot fluids circulation (JICA – EPEN 1992). The
433 geometries of the DDS's, as defined by the φCO₂ distribution, **are roughly** consistent with
434 these three directions (Fig. 5). In particular at Termas de Copahue, Las Maquinitas I and II
435 the high CO₂ fluxes **seem to be** mainly distributed along the NE-SW-aligned structures,
436 which correspond to either known faults or faults inferred by this investigation **on the basis**
437 of diffuse degassing processes active in this area. At Las Máquinas, the DDS develops

438 along both NE-SW and WNW-ESE structural trends. The general correspondence between
439 the structural trends and the DDSs geometries suggests that the emission of the
440 hydrothermal fluids is favored by the fault systems, which cut through the vapor zone,
441 causing the transfer of the deep fluids towards the surface. In Figure 5, the extension of
442 such vapor zone was roughly delimited: the studied DDS would be located in the northern
443 and eastern limits of this "hot area" with the exception of Anfiteatro which, according to
444 this hypothesis, would be positioned externally with respect to the "hot area". This is
445 supported by the chemical and isotopic composition of the fumarolic fluids discharged at
446 Anfiteatro, as they significantly differ from the other areas. The Anfiteatro fumaroles are
447 indeed richer in water ($\text{H}_2\text{O}/\text{CO}_2$ molar ratio of ~ 100) and the $^3\text{He}/^4\text{He}$ ratio is significantly
448 lower ($R/R_a \sim 4.9$) than those measured at Las Máquinas, Las Maquinitas and Piedra
449 Copahue.

450

451 **4.4 Estimation of the thermal energy release**

452 At the Copahue hydrothermal sites, the thermal energy release was estimated by
453 using an approach similar to that **described in** Chiodini et al. (2001; 2005). The
454 computation was based on (i) the estimation of the **pristine** $\text{H}_2\text{O}/\text{CO}_2$ ratio ($R_{\text{H}_2\text{O}-\text{CO}_2}$ by
455 weight) of the fluid feeding the soil diffuse gas emission before steam condensation and (ii)
456 the computation of the total steam involved in the process Q_{steam} by multiplying $Q_{\text{CO}_2,d}$ by
457 $R_{\text{H}_2\text{O}-\text{CO}_2}$. In the case of Las Maquinitas, **the** measured fumarolic CO_2 flux (3.2 t d^{-1}) **was**
458 **added to the diffuse CO_2 output**. In each hydrothermal site, Q_{steam} was computed with the
459 reasonable assumption that $R_{\text{H}_2\text{O}-\text{CO}_2}$ is equal to the $\text{H}_2\text{O}/\text{CO}_2$ ratio measured in the
460 fumaroles of the correspondent degassing structure (Table 5). The total amount of steam
461 from each area (Q_{steam}) varies from 285 t d^{-1} at La Maquinitas to $1,506 \text{ t d}^{-1}$ at Termas de
462 Copahue (Table 5). The total thermal release QH_{tot} (Table 5) was calculated by adding
463 three contributions:

464 1) QH_{res} **represents** the heat released by the $\text{H}_2\text{O}-\text{CO}_2$ gas mixture moving **from the**
465 **reservoir conditions to the condensation zone**. The reservoir temperatures **were**
466 **considered equal to $210 \text{ }^\circ\text{C}$** , whilst the reservoir pressure was **assumed that of the**
467 **saturated vapor at which P_{CO_2}** , computed by multiplying $P_{\text{H}_2\text{O}}$ by the measured
468 fumarolic $\text{CO}_2/\text{H}_2\text{O}$ molar **ratio, was added**. QH_{res} was calculated by multiplying Q_{steam}

469 by the enthalpy difference between the vapor at reservoir conditions and at
470 condensation conditions (0.096 Mpa and 98 °C). The computation was performed using
471 MUFITS software, which allows to predict CO₂-H₂O mixture properties in a wide range
472 of pressures and temperatures (Afanasyev, 2013). QH_{res} ranges from 0.5 MW to 3.6
473 MW, thus it is the minor term of the energetic balance of the diffuse degassing
474 structures (Table 5);

475 2) QH_{cond} corresponds to the heat released during steam condensation at subsurface
476 conditions. The QH_{cond} values, which were computed by multiplying Q_{steam} by the latent
477 heat of condensation at 98 °C (2,262 J g⁻¹), range from 7.5 MW at Las Maquinitas I and
478 II areas to 39.4 MW at Termas de Copahue (Table 5). QH_{cond} is the main term of the
479 energy budget;

480 3) QH_{cooling} is the heat released as the condensates cool down to ambient temperature. It
481 was estimated by multiplying Q_{steam} by the enthalpy difference between the liquid at 98
482 °C (enthalpy = 411 j g⁻¹) and at 10 °C (enthalpy = 42 j g⁻¹). The QH_{cooling} values, from
483 1.2 to 6.4 MW, were intermediate between those of QH_{res} and QH_{cond} (Table 5).

484 The total thermal energy release from the five-surveyed zones is 107.5 MW. The highest
485 thermal energy release (49.1 MW) was estimated at Termas de Copahue, where the
486 computed Q_{steam} was 1,506 t/d. Here, the production of large amount of condensates is
487 shown by the mass balance calculated for the small creek (Rio Frio, Fig. 1) that enters the
488 village with a flow rate of 560 t d⁻¹ (pH = 6.06, T = 16.2 °C), collects the great majority of
489 the condensation waters and flows out at the rate of 1,460 t d⁻¹ (pH = 3.4, T = 22.5 °C).
490 The measured flow rate increment, which is about 60% of the estimated condensate
491 production in the area, appears to be realistically supporting the reliability of our
492 estimation. It is indeed reasonable that part of the condensates is feeding the local aquifer
493 (groundwater circulation).

494 **Table 5.** Heat flux estimation.

495 **6. Conclusions**

496 The north-western sector of the Caviahue caldera is characterized by fumarolic
497 emissions associated with zones of anomalously high soil CO₂ diffuse degassing and soil
498 temperature. Five of these sites were investigated and a total discharge of deeply-originated

499 CO₂ of ~165 t d⁻¹ from soil diffuse degassing processes was estimated. The gas source for
500 Termas de Copahue, Las Máquinas, Las Maquinitas I and II is a 800-1,000 m deep vapor
501 zone with a temperature of ~200-215 °C, as indicated by both the data of three deep wells
502 drilled in the eighties SW of the natural degassing sites, and gas geothermometry. The
503 occurrence of a unique gas zone feeding the manifestations of the area explains the
504 remarkable compositional homogeneity of the fumaroles, with the exception of those
505 discharging at Anfiteatro, where significant compositional and isotopic differences with
506 respect to the other sites were observed. Using CO₂ as a tracer of the original vapor phase, a
507 natural thermal release of ~77 MW from Termas de Copahue, Las Máquinas, Las
508 Maquinitas I and II was computed, and increases up to ~107 MW when the Anfiteatro
509 degassing zone is considered.

510 The clear magmatic signature of the incondensable fumarolic gases, the wide
511 expanse of the hydrothermal zones and the remarkable amount of gas and heat released by
512 fluid expulsion, appear to be compatible with an active magmatic intrusion in the
513 subsurface of this portion of the Caviahue caldera. This model well agrees with the proved
514 occurrence of volcanic seismic tremor associated with the hydrothermal systems of the
515 Copahue-Caviahue Volcanic Complex (Ibañez et al. 2008; Forte et al. 2012).

516

517 **Acknowledgements**

518 The research leading to these results has received funding from Deep Carbon
519 Observatory under the DECADE research initiative (sub-contract 10470-1145), from the
520 projects UBACyT 01-W172 and UBACyT 20020120300077BA, PI UNRN 40-A-294 and
521 PI UNRN 40-A-379. This paper benefitted the useful and helpful comments of two
522 anonymous reviewers who improved an early version of the manuscript.

523 **References**

- 524 Afanasyev A.A. (2013). Multiphase compositional modelling of CO₂ injection under
525 subcritical conditions: The impact of dissolution and phase transitions between liquid and
526 gaseous CO₂ on reservoir temperature. *Int. J. Greenhouse Gas Control* 19, 731–742.
527 <http://dx.doi.org/10.1016/j.ijggc.2013.01.042>.
- 528 Augusto M. (2011). Estudio geoquímico de los fluidos volcánicos e hidrotermales del
529 Complejo Volcánico Copahue Caviahue y su aplicación para tareas de seguimiento. Tesis
530 Doctoral (unpublished). Universidad de Buenos Aires. 290 p.
- 531 Augusto M., Caselli A., Tassi F., Dos Santos Alfonso M., Vaselli O. (2012). Seguimiento
532 geoquímico de las aguas ácidas del sistema volcán Copahue-Río Agrio: posible aplicación
533 para la identificación de precursores eruptivos. *Revista de la Asociación Geológica*
534 *Argentina* 69 (4): 481-495.
- 535 Augusto M., Tassi F., Caselli A., Vaselli O., Rouwet D., Capaccioni B., Caliro S., Chiodini
536 G., Darrah T. (2013). Gas geochemistry of the magmatic-hydrothermal fluid reservoir in the
537 Copahue-Caviahue Volcanic Complex (Argentina). *Journal of Volcanology and*
538 *Geothermal Research* 257, 44-56.
- 539 Burton M.R., Sawyer G.M., Granieri D. (2013). Deep Carbon Emissions from Volcanoes.
540 *Reviews in Mineralogy & Geochemistry*. Vol. 75 pp. 323-354. doi:
541 10.2138/rmg.2013.75.11
- 542 Bermúdez A., Delpino D., López Escobar L. (2002). Caracterización geoquímica de lavas y
543 piroclastos holocenos del volcán Copahue, incluyendo los originados en la erupción del año
544 2000. Comparación con otros volcanes de la Zona Volcánica Sur de los Andes. XV
545 Congreso Geológico Argentino, Calafate. Actas 1, 377-382.
- 546 Berner R.A., Lasaga A.C. (1989). Modeling the geochemical carbon cycle. *Scientific*
547 *American* 260:74-81.
- 548 Bloomberg S., Werner C., Rissmann C., Mazot A., Horton T., Gravley D., Kennedy B.,
549 Oze C. (2014). Soil CO₂ emissions as a proxy for heat and mass flow assessment, Taupo
550 Volcanic Zone, New Zealand. *Geochemistry Geophysics Geosystems* 15, 4885–4904,
551 doi:10.1002/2014GC005327.
- 552 Cardellini C., Chiodini G., Frondini F. (2003). Application of stochastic simulation to CO₂
553 flux from soil: mapping and quantification of gas release. *Journal of Geophysical Research*
554 108:2425. doi:10.1029/2002JB002165.

555 Caselli A., Agosto M., Fazio A. (2005) Cambios térmicos y goequímicos del lago cratérico
556 del volcán Copahue (Neuquén): posibles variaciones cíclicas del sistema volcánico. XVI
557 Congreso Geológico Argentino, T1, 751-756.

558 Caselli A., Agosto M., Velez M.L., Forte P., Bengoa C., Daga R., Albite J.M., Capaccioni
559 B. (2015). The 2012 eruption. In Tassi F., Vaselli O., Caselli A. (ed) Copahue Volcano:
560 The smoking mountain between Argentina y Chile. Springer International Publishing AG.
561 (Accepted).

562 Chiodini, G., Cioni, R., Guidi, M., Marini, L., Raco, B. (1998). Soil CO₂ measurements in
563 volcanic and geothermal areas. *Applied Geochemistry*, 13:543–552.

564 Chiodini G., Frondini F., Cardellini C., Granieri D., Marini L., Ventura G. (2001). CO₂
565 degassing and energy release at Solfatara volcano, Campi Flegrei, Italy. *Journal of*
566 *Geophysics Research: Solid Earth* 106:16,213-16,221, doi: 10.1029/2001JB000246.

567 Chiodini G., Granieri D., Avino R., Caliro S., Costa A., Werner C. (2005). Carbon dioxide
568 diffuse degassing and estimation of heat release from volcanic and hydrothermal systems.
569 *Journal of Geophysics Research: Solid Earth* 110:B08204, doi: 10.1029/2004JB003542.

570 Chiodini G., Baldini A., Barbieri F., Carapezza M., Cardellini C., Frondini F., Granieri D.,
571 Ranaldi M. (2007). Carbon dioxide degassing at Latera caldera (Italy): evidence of
572 geothermal reservoir and evaluation of its potential energy. *Journal of Geophysics*
573 *Research*. doi:10.1029/2006JB004896.

574 Chiodini G., Caliro S., Cardellini C., Avino R., Granieri D., Schmidt A. (2008). Carbon
575 isotopic composition of soil CO₂ efflux, a powerful method to discriminate different
576 sources feeding soil CO₂ degassing in volcanic-hydrothermal areas. *Earth and Planetary*
577 *Science Letters*, 274 (3-4), pp. 372-379.

578 Chiodini G., Vandemeulebrouck J., Caliro S., D' Auria L., De Martino P., Mangiacapra A.,
579 Petrillo Z. (2015). Evidence of thermal-driven processes triggering the 2005–2014 unrest
580 at Campi Flegrei caldera. *Earth and Planetary Science Letters* 414, 58–67.
581 doi:10.1016/j.epsl.2015.01.012

582 Dellapé D., Pando G. (1975). Relevamiento geológico de la cuenca geotérmica de
583 Copahue. Yacimientos Petrolíferos Fiscales. Unpublished Report No. 524, pp. 11.

584 Delpino D., Bermúdez A. (1993). La actividad del volcán Copahue durante 1992. Erupción
585 con emisiones de azufre piroclástico. Provincia de Neuquén, Argentina. XII Congreso
586 Geológico Argentino y II Congreso de Exploración de Hidrocarburos. Actas 4, 292-301.

- 587 Delpino D., Bermúdez A. (2002). La erupción del volcán Copahue del año 2000. Impacto
588 social y al medio natural 15° Congreso Geológico Argentino. Actas 3: 365-370.
- 589 DeMets C., Gordon R., Argus F., Stein S. (1994). Effect of recent revisions of the
590 geomagnetic time scale on estimates of current plate motions. *Geophysical Research*
591 *Letters* 21, 2191-2194.
- 592 Deutsch C.V., Journel A.G. (1998). *Geostatistical Software Library and User's Guide*, 2nd
593 ed. Oxford University Press, New York.
- 594 **Dionis, S.M., Melián, G., Rodríguez, F., Hernández, P., Padrón, E., Pérez, N., Barrancos,**
595 **J., Padilla, G., Sumino, H., Fernandes, P., Bandomo, Z., Silva, S., Pereira, J., Semedo, H.**
596 **(2015). Diffuse volcanic gas emission and thermal energy release from the summit crater of**
597 **Pico do Fogo, Cape Verde. *Bulletin of Volcanology*. doi: 10.1007/s00445-014-0897-4.**
- 598 Folguera A., Ramos V., Hermanns R., Naranjo J. (2004). Neotectonics in the foothills of
599 the Southernmost Central Andes (37°-38°S). Evidence of the strike-slip displacement along
600 the Antiñir-Copahue fault zone. *Tectonics* 23 TC 5008 23 pp.
- 601 Folguera A., Zapata T., Ramos V. (2006). Late Cenozoic extension and evolution of the
602 Neuquén Andes. In Kay S., Ramos V. (ed) *Evolution of the Andean margin: A tectonic and*
603 *magmatic view from the Andes to the Neuquén basin (35°-39°S)*. GSA Special Paper, 407.
- 604 Forte P., Bengoa C., Caselli A. (2012). Análisis preliminar de la actividad sísmica del
605 complejo volcánico Copahue-Caviahue mediante técnicas de array. 13° Congreso
606 Geológico Chileno, acts: 574-576.
- 607 Fridriksson T., Kristjansson B.R., Armannsson H., Margretardottir E., Olafsdottir S.,
608 Chiodini G. (2006) CO₂ emissions and heat flow through soil, fumaroles, and steam-heated
609 mud pools at the Reykjanes geothermal area, SW Iceland, *Applied Geochemistry* 21, 1551–
610 1569. doi:10.1016/j.apgeochem.2006.04.006.
- 611 Giggenbach W.F. (1975). A simple method for the collection and analysis of volcanic gas
612 samples. *Bulletin of Volcanology* 39 (1): 132–145.
- 613 Giggenbach W.F., Goguel R.L. (1989). *Methods for the collection and analysis of*
614 *geothermal and volcanic water and gas samples*. Department of Scientific and Industrial
615 Research, Chemistry Division, Report 2401.
- 616 Giggenbach W.F., and Matsuo S. (1991). Evaluation of results from Second and Third
617 IAVCEI field workshops on Volcanic gases, Mt. Usu, Japan, and White Island, New
618 Zealand. *Applied Geochemistry* 6 (2): 125–141.

619 Granirei D., Giovanni C., Avino R., Caliro S. (2014). Carbon dioxide emission and heat
620 release estimation for Pantelleria Island (Sicily, Italy), *Journal of Volcanology and*
621 *Geothermal Research* 275: 22–33. doi: 10.1016/j.jvolgeores.2014.02.011

622 GVN 2000a. Bulletin of the Global Volcanism Network. Volcanic Activity Reports. Vol.
623 25. N° 6. pp: 10-14.

624 GVN 2000b. Bulletin of the Global Volcanism Network. Volcanic Activity Reports. Vol.
625 25. N° 9. pp: 1-3.

626 Hernández P.A., Pérez N.M., Fridriksson T., Egbert J., Ilyinskaya E., Thárhallsson A.,
627 Ívarsson G., Gíslason G., Gunnarsson I., Jónsson B. (2012). Diffuse volcanic degassing and
628 thermal energy release from Hengill volcanic system, Iceland. *Bulletin of Volcanology* 74:
629 2435-2448.

630 Ibáñez J.M., Del Pezzo E., Bengoa C., Caselli A., Badi G., Almendros J. (2008). Volcanic
631 tremor and local earthquakes at Copahue volcanic complex, Southern Andes, Argentina.
632 *Journal of Volcanology and Geothermal Research* 174 (2008) 284–294.

633 JICA-EPEN (Japan International Cooperation Agency) (1992) The feasibility study on the
634 Northern Neuquén Geothermal Development Project (Unpublished). Ente Provincial de
635 Energía de la Provincia de Neuquén 89 p.

636 Jurío R.L. (1977). Características geoquímicas de los fluidos termales de Copahue
637 (Neuquén - Argentina). Principales implicancias geotérmicas. *Minería* 172, 11 pp.

638 Latinoconsult (1981). Estudio de Pospección Geotérmica en el área de Copahue. COPADE,
639 Neuquén.

640 Lavenu A., Cembrano J. (1999). Compressional and transpressional stress pattern for
641 Pliocene and Quaternary brittle deformation in fore-arc and intra-arc zones (Andes of
642 Central and Southern Chile). *Journal of Structural Geology* 21: 1669-1691.

643 Lewicki J.L., Bergfeld D., Cardellini C., Chiodini G., Granieri D., Varley N., Werner C.
644 (2005). Comparative soil CO₂ flux measurements and geostatistical estimation methods on
645 Masaya volcano, Nicaragua. *Bulletin of Volcanology* 68 (1): 76-90.

646 Lewicki J.L., Oldenburg C.M. (2005). Near-Surface CO₂ Monitoring and analysis to detect
647 hidden geothermal systems. PROCEEDINGS, Thirtieth Workshop on Geothermal
648 Reservoir Engineering. Stanford University SGP-TR-176.

649 Martini M., Bermúdez A., Delfino D., Giannini L. (1997). The thermal manifestation of
650 Copahue volcano area. Neuquen. Argentina. VIII Congreso Geológico Chileno,
651 Antofagasta 4: 352-356.

- 652 Mas G.R., Mas L.C., Bengochea L. (1996). Alteración ácido-sulfática en el Campo
653 Geotérmico Copahue, Provincia del Neuquén. *Asociación Geológica Argentina* 51 (1): 78-
654 86.
- 655 Mas L.C., Mas G.R., Bengochea L. (2000). Heatflow of Copahue geothermal field, its
656 relation with tectonic scheme. *Proceedings of World Geothermal Congress, Tohoku, Japan*
657 pp. 1419-1424.
- 658 Mazot A., Taran Y. (2009). CO₂ flux from the volcanic lake of El Chichón (Mexico):
659 *Geofísica Internacional* 48 (1):73-83.
- 660 Melnick D., Folguera A., Ramos V.A. (2006). Structural control on arc volcanism: The
661 Copahue-Agrio complex, South-Central Andes (37°50'S). *Journal of South American Earth*
662 *Sciences* 22: 66-88.
- 663 Naranjo J.A., Polanco E. (2004). The 2000 AD eruption of Copahue Volcano, Southern
664 Andes. *Revista Geológica de Chile*, 31 (2): 279-292.
- 665 Panarello H., Levin M., Albero M.C., Sierra J.L., Gingins M.O. (1988). Isotopic and
666 geochemical study of the vapor dominated geothermal field of Copahue (Neuquén,
667 Argentina). *Revista Brasileira de Geofísica* 5 (2): 275-282.
- 668 Panarello H. (2002). Características isotópicas y termodinámicas de reservorio del campo
669 geotérmico Copahue-Caviahue, provincia del Neuquén. *Revista de la Asociación Geológica*
670 *Argentina* 57 (2): 182-194.
- 671 Pesce A. (1989). Evolución volcano-tectónica del complejo efusivo Copahue-Caviahue y su
672 modelo geotérmico preliminar. *Revista de la Asociación Geológica Argentina*, 44 (1-4):
673 307-327.
- 674 Polanco E. (2003). Evolución del volcán Copahue (37° 45' S), Andes del Sur. Tesis de
675 Maestría (unpublished), Universidad Nacional Autónoma de México, 90 p.
- 676 Radic J.P. (2010). Las cuencas cenozoicas y su control en el volcanismo de los complejos
677 Nevados de Chillán y Copahue-Callaqui (36°-39°S). *Andean Geol* 37(1): 220-246.
- 678 Ramos V.A., Folguera A. (2000). Tectonic evolution of the Andes of Neuquén: constraints
679 derived from the magmatic arc and foreland deformation. In Veiga GD, Spalletti LA,
680 Howell JA, Schwartz E (eds.) *The Neuquén Basin, Argentina: A Case Study in Sequence*
681 *Stratigraphy and Basin Dynamics: Geological Society, London, Special Publications*, 252:
682 15–35.
- 683 Raich J.W., Schlesinger W.H. (1992). The global carbon dioxide flux in soil respiration and
684 its relationship to vegetation and climate, *Tellus*, 44B: 81-99.

- 685 Raich J.W., Tufekcioglu A. (2000). Vegetation and soil respiration: Correlations and
686 controls. *Biogeochemistry* 48(1): 71-90.
- 687 Rissmann C., Christenson B., Werner C., Leybourne M., Cole J., Gravley D. (2012).
688 Surface heat flow and CO₂ emissions within the Ohaaki hydrothermal field, Taupo
689 Volcanic Zone, New Zealand, *Applied Geochemistry* 27: 223–239.
690 doi:10.1016/j.apgeochem.2011.10.006.
- 691 Rojas Vera E.A., Folguera A., Zamora Valcarce G., Giménez M., Ruiz F., Martínez P.,
692 Bottesi G., Ramos V.A. (2010). Neogene to Quaternary extensional reactivation of a fold
693 and thrust belt: the Agrio belt in the Southern Central Andes and its relation to the
694 Loncopué trough (38°–39°S). *Tectonophysics* 92 (1–4): 279–294.
- 695 Sierra J., D'Amore F., Panarello H., Pedro G. (1990). Reservoir characteristics of the
696 vapour dominated geothermal field of Copahue, Neuquén, Argentina, as established by
697 isotopic and geochemical techniques. *Geothermal Investigations with Isotope and
698 Geochemical Techniques in Latin America. Final Proc. Nuclear Techniques in Geothermal
699 Resources Investigation, San José, Costa Rica*, pp. 13–30.
- 700 Sinclair A.J. (1974). Selection of threshold values in geochemical data using probability
701 graphs, *Journal of Geochemical Exploration* 3: 129– 149.
- 702 Tamburello G., Agosto M., Caselli A., Tassi F., Vaselli O., Calabrese S., Rouwet D,
703 Capaccioni B., Cardellini C., Chiodini G., Di Napoli R., Liccioli C., Bitetto M., Brusca L.,
704 Bellomo S., Aiuppa A. (2015). Intense magmatic gas leakage through the Copahue crater
705 lake. *Journal of Geophysical Research, in press*.
- 706 Tassi F., Agosto M., Vaselli O., Chiodini G. (2015). Geochemistry of the magmatic-
707 hydrothermal fluid reservoir of Copahue volcano (Argentina): insights from the chemical
708 and isotopic features of fumarolic discharges. En Tassi F, Vaselli O, Caselli A (ed)
709 Copahue Volcano: The smoking mountain between Argentina y Chile. Springer
710 International Publishing AG. (Accepted).
- 711 Varekamp J.C., Ouimette A., Hermán S., Bermúdez A., Delpino D. (2001). Hydrothermal
712 element fluxes from Copahue, Argentina: A "beehive" volcano in turmoil. *Geology* 29 (11):
713 1059-1062.
- 714 Werner C., Cardellini C. (2006). Comparison of carbon dioxide emissions with fluid
715 upflow, chemistry, and geologic structures at the Rotorua geothermal system, New
716 Zealand, *Geothermics* 35: 221–238. doi:10.1016/j.geothermics.2006.02.006.
- 717 Yuan X., Asch G., Bataille K., Bock G., Bohm M., Echtler H., Kind R., Oncken O.,
718 Wölbern I. (2006). Deep seismic images of the Southern Andes. In Kay S. Ramos VA (ed)

- 719 Evolution of the Andean Margin: a tectonic and magmatic view from the Andes to the
720 Neuquen basin (35° - 39°S). GSA Special Paper 407: 61-72.

Table 1. Chemical composition of the fumaroles of the surveyed areas (March 2012). Gas concentrations are expressed in $\mu\text{mol/mol}$, helium isotopes as R/Ra ($^3\text{He}/^4\text{He}_{\text{sample}}/^3\text{He}/^4\text{He}_{\text{air}}$). Equilibrium temperatures were calculated within the $\text{H}_2\text{O}-\text{H}_2-\text{CO}_2-\text{CO}-\text{CH}_4$ gas system ($T_{\text{H-C-O}}$; Tassi et al., 2015) and the geothermometer based on the CO/CO_2 ratio ($T_{\text{CO-CO}_2}$; Chiodini et al., 2015).

Name	T °C	H ₂ O	CO ₂	H ₂ S	N ₂	CH ₄	H ₂	He	CO	R/Ra	T _{H-C-O} °C	T _{CO-CO₂} °C
Las Máquinas	96	973000	25200	189	511	540	395	0.32	0.057	7.04	203	206
Las Maquinitas I	130	976000	23100	214	521	290	312	0.32	0.049	6.97	210	204
Termas de Copahue	95	975000	24100	212	449	286	319	0.30	0.052	7.01	210	204
Anfiteatro	92	989000	9470	213	4045	641	184	0.24	0.068	4.93	258	244

Table 2. Main parameters of the five surveyed areas.

Name	Extension (m ²)	No. of points	Mean (min-max) ϕCO_2 (g m ⁻² d ⁻¹)
Las Máquinas	320,823	495	145 (<0.05 – 7,270)
Las Maquinitas I	45,842	141	78 (<0.05 – 2,200)
Las Maquinitas II	32,802	103	272 (<0.05 – 14,330)
Anfiteatro	26,089	346	105 (<0.05 – 16,560)
Termas de Copahue	575,748	678	195 (<0.05 – 9,380)
Total	1,212,585	1763	158 (<0.05 – 16,560)

Table 3. Estimated parameters and partitioned populations in the 5 surveyed areas.

Name	Population	Proportion (%)	Average ϕCO_2 and 90% confidence interval ($\text{g m}^{-2} \text{d}^{-1}$)	Total diffuse CO_2 output and 90% confidence interval (t d^{-1})
Las Máquinas	A (background)	8	1.01 (0.82 - 1.23)	0.03 (0.02 - 0.03)
	B (background)	78	24 (22 - 27)	5.9 (5.3 - 6.6)
	C (endogenous)	12	388 (276 - 538)	15 (11 - 21)
	D (endogenous)	2	4,379 (3,058 - 6,038)	28 (20 - 39)
	Total	100		49 (36 - 66)
Las Maquinitas I	A (endogenous)	100	95 (49 - 181)	4.4 (2.2 - 8.3)
La Maquinitas II	A (background)	55	4.9 (4 - 6)	0.09 (0.07 - .11)
	B (endogenous)	37	86 (56 - 128)	1 (0.7 - 1.6)
	C (endogenous)	8	5,815 (1,298 - 1,5995)	15.3 (3.4 - 42)
	Total	100		16 (4 - 44)
Anfiteatro	A (background)	12.5	<0.1	nd
	B (background)	40.5	6.7 (5.2 - 8.7)	0.64 (0.49 - 0.83)
	C (background)	44	26 (21 - 32)	2.7 (2.2 - 3.3)
	D (endogenous)	3	5,634 (1,213 - 15,022)	40 (9 - 106)
	Total	100		43 (11 - 110)
Termas de Copahue	A (background)	8	0.99 (0.89 - 1.10)	0.05 (0.04 - 0.05)
	B (background)	73	22 (19 - 25)	9.2 (8.1 - 10.4)
	C (endogenous)	19	1,000 (784 - 1,270)	109 (86 - 139)
	Total	100		119 (94 - 174)

Table 4. Relevant parameters of SGS application and estimation of the total CO₂ output from Copahue hydrothermal sites.

Site name	Variogram model, nugget, range (m)	Grid parameters: n.cells, lag (m)	Total CO₂ release ± standard deviation (t d-1)	Endogenous CO₂ release, Q_{CO2} (t d-1)
Las Máquinas	Spherical, 0.47, 145	35647, 3	42.7 ± 4.33	36.8
Las Maquinitas I	Spherical, 0.51, 50	45842, 1	5.01 ± 0.81	5.0(1)
Las Maquinitas II	Spherical, 0.46, 66	32802, 1	8.30 ± 1.56	8.3
Anfiteatro	Spherical, 0.71, 80	29748, 3	24.0 ± 2.45	21.7
Termas de Copahue	Spherical, 0.59, 194	63972, 3	100 ± 5.42	90.8
Total	-	-	180	162.6

(1) At Las Maquinitas I, an additional CO₂ flux of ~ 3.2 t d-1 was measured from the main fumarolic vent.

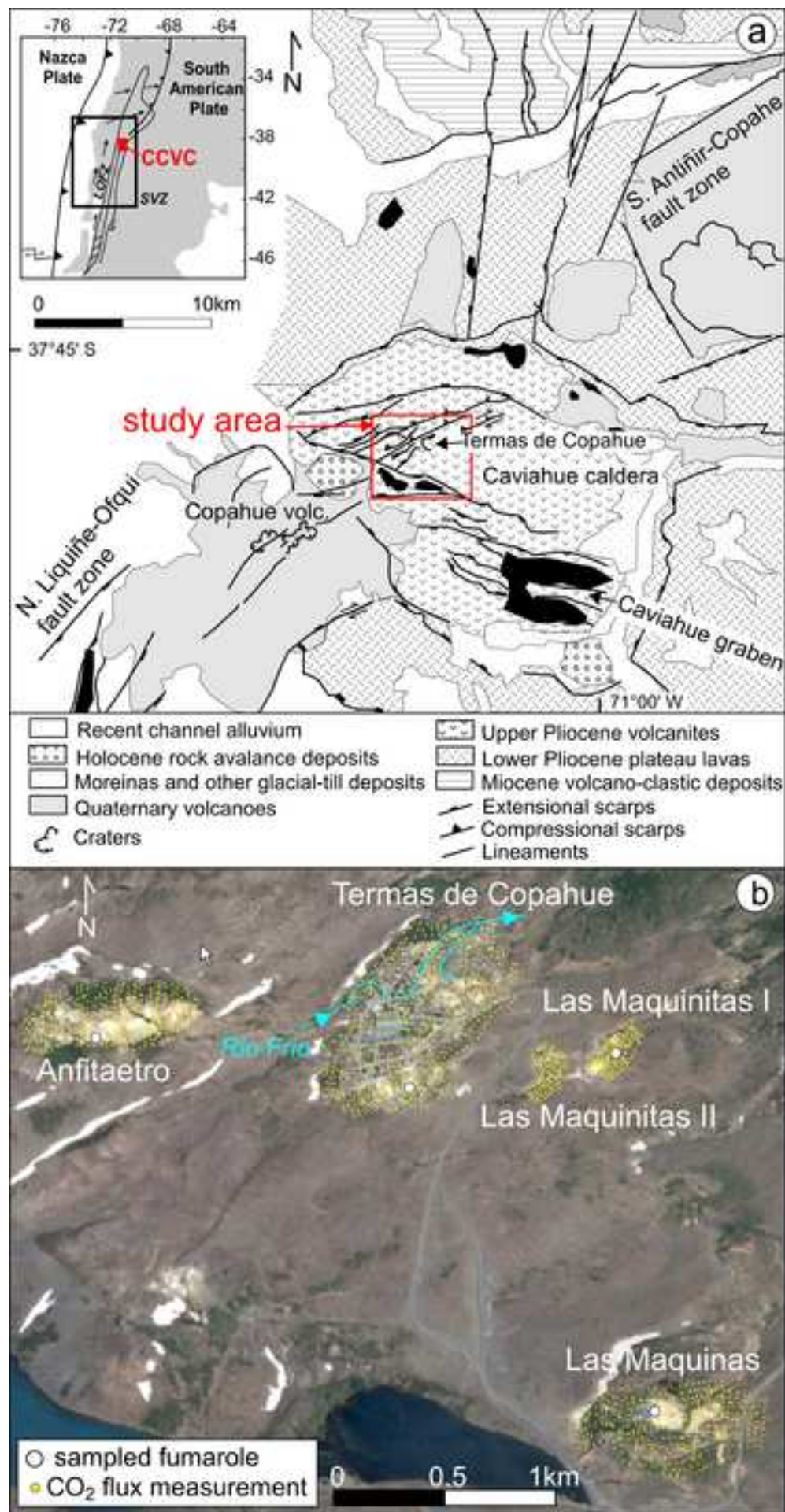
Table 5. Heat flux estimation.

Hydrothermal site	R_{H₂O-CO₂}	Q_{steam} (t d⁻¹)	QH_{res} (MW)	QH_{cond} (MW)	QH_{cooling} (MW)	QH_{tot} (MW)
Las Máquinas	15.8	581	1.2	15.2	2.5	18.9
Las Maquinitas I, II ⁽¹⁾	17.3	285	0.5	7.5	1.2	9.1
Termas de Copahue	16.6	1506	3.2	39.4	6.4	49.1
Anfiteatro	42.7	927	2.2	24.3	4.0	30.4
Total	-	3244				107.5

⁽¹⁾ At Las Maquinitas Q_{steam} includes the contribution of the main fumarolic vent which was computed in 55 t d⁻¹ by multiplying the measured CO₂ flux (3.2 t d⁻¹) by R_{H₂O-CO₂}.

Figure

[Click here to download high resolution image](#)



Figure

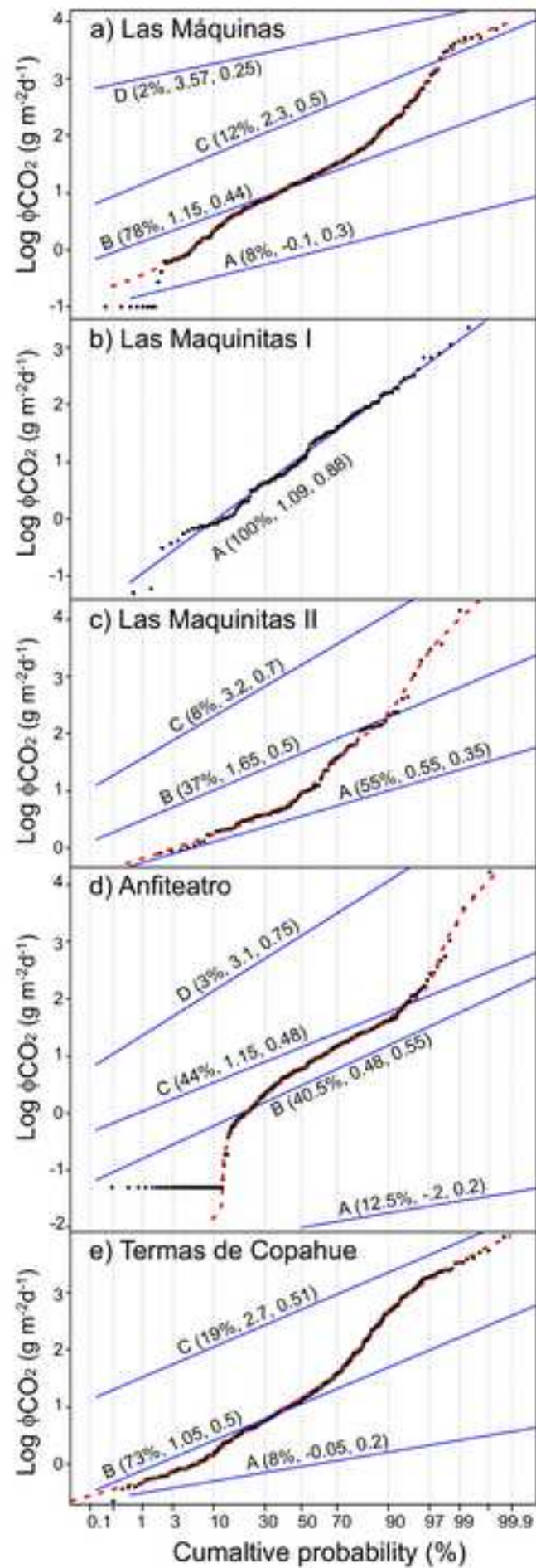
[Click here to download high resolution image](#)

Figure
[Click here to download high resolution image](#)

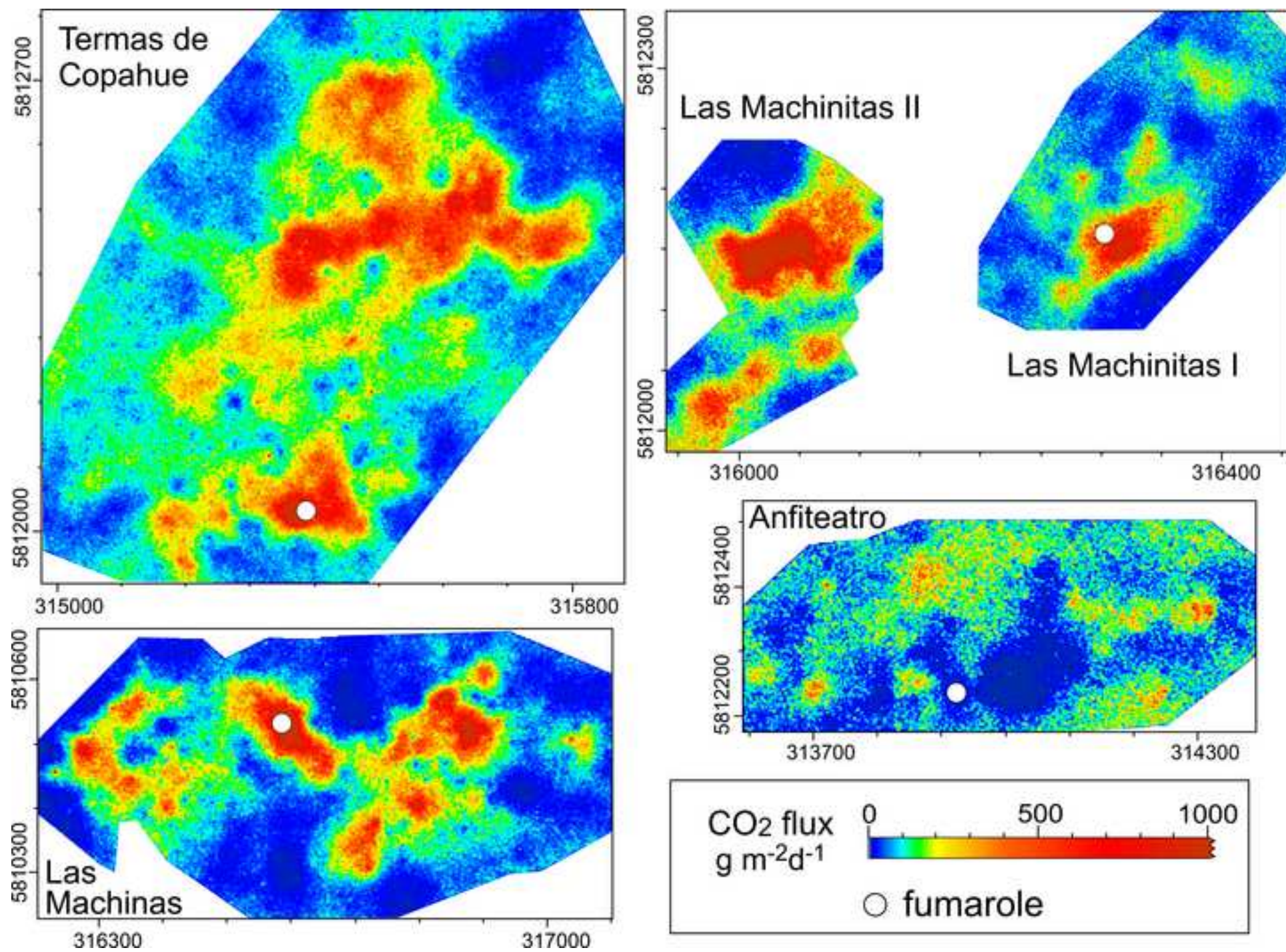
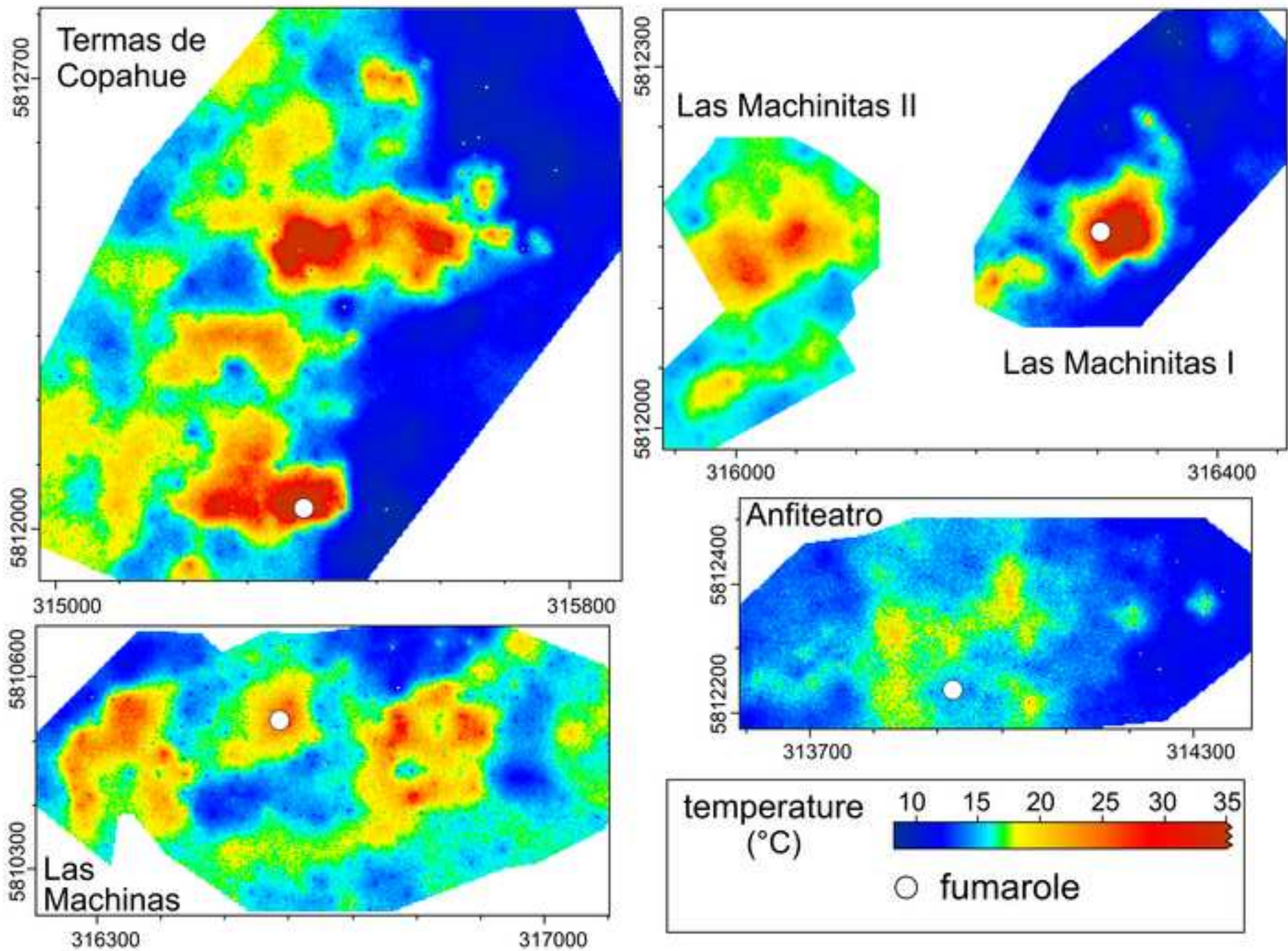


Figure
[Click here to download high resolution image](#)



Figure

[Click here to download high resolution image](#)

